(This is a sample cover image for this issue. The actual cover is not yet available at this time.)

International Journal of Heat and Mass Transfer 59 (2013) 262–271

Contents lists available at SciVerse ScienceDirect

International Journal of Heat and Mass Transfer

journal homepage: www.elsevier.com/locate/ijhmt

Adsorbate uptake and mass diffusivity of working pairs in adsorption cooling systems

Amir Sharafian, Majid Bahrami *

Laboratory for Alternative Energy Conversion (LAEC), Mechatronic Systems Engineering, Simon Fraser University, BC, Canada V3T 0A3

ARTICLE INFO

Article history:
Received 11 October 2012
Received in revised form 8 December 2012
Accepted 8 December 2012

Keywords:
Adsorbate uptake rate
Mass diffusivity
RC model
Solid-side resistance

ABSTRACT

A new closed-form model is proposed to determine the adsorbate uptake rate and the mass diffusivity of adsorbent–adsorbate pairs using experimental data of the gravimetric method based on the concept of Resistance–Capacitance (RC) analogy. The present model is verified against the available analytical solution for the adsorbate uptake for spherical micropore adsorbent particles with solid-side resistance on the surface of adsorbent. Furthermore, a new closed-form relationship for adsorbate uptake rate during the adsorption/desorption processes in adsorption cooling systems (ACS) is developed based on the linear driving force (LDF) model. The proposed adsorbate uptake rate relationship is applicable to the entire range of mass transfer Biot numbers and is as convenient-to-use as the LDF adsorbate uptake rate model. Moreover, the present model can be used to determine the mass diffusivity of spherical micropore adsorbent–adsorbate pairs with less computational time than that of the analytical series solution.

1. Introduction

Diffusion in micropore and mesopore materials is a dominant process in a wide range of applications such as gas separation and purification [1,2], petrochemical processes [3,4], industrial air pollution control [5], air dehumidification in air conditioning systems [6,7], food industries [8–10] and biomechanics [11,12]. An emerging application of micropore and mesopore materials is in adsorption cooling systems (ACS) for air conditioning in buildings and automotive industries which have received an immense attention in the recent years mainly due to higher fuel prices, energy shortages, and stringent governmental environmental/emission regulations [13–15]. Conventional vapor compression refrigeration cycle (VCRC), used in automotive air conditioning systems, consumes a considerable power of the engine [16] to derive the compressor, which significantly increases fuel consumption. A VCRC compressor can add up to 5–6 kW peak power draw on a vehicle's engine that is equivalent to the power required for a 1200-kg sedan cruising at 60 km/h [16]. In a conventional internal combustion engine (ICE), almost 40% of the total fuel energy is dissipated through the exhaust gas of the engine [16] in the form of waste heat. A portion of this waste heat is sufficient to run an ACS to meet the air-conditioning of a vehicle. Proper implementation of ACS in automobiles can significantly reduce the fuel consumption and minimize the carbon footprint of vehicles.

Working pairs in ACS are a combination of a sorbent material, called adsorbent, such as zeolite, silica gel and activated carbon; and a refrigerant, called adsorbate, such as water and methanol. These materials are environmentally friendly, non-toxic, non-corrosive, and inexpensive. Moreover, ACS are quiet and easy to maintain. As such, ACS are ideal candidates for conventional VCRC. However, commercialization of ACS faces major challenges; namely: (i) low specific cooling power (SCP) and (ii) poor coefficient of performance (COP) that result in heavy and bulky air-conditioning systems, which are not practical for automotive applications. Specific cooling power is the ratio of cooling power to the mass of dry adsorbent times the cycle time. Thus, SCP can be maximized by decreasing the adsorbent mass and/or reducing the cycle time. The origins of these limitations are low mass diffusivity and thermal conductivity of the adsorbent–adsorbate pairs. To improve SCP, the following approaches can be adopted:

- Improving thermal conductivity of working pairs by using new synthetic materials such as carbon nanotubes (CNT) embedded in zeolite [17].
- Increasing effective surface area of adsorber bed to increase the heat transfer rate between the exhaust gas (waste heat) and the adsorbent particles.
- Reducing cycle time by increasing adsorbate diffusion rate within the adsorbent particles during the adsorption/desorption processes.

* Corresponding author. Address: Mechatronic Systems Engineering, Simon Fraser University, #4300, 250-13450 102nd Avenue, Surrey, BC, Canada V3T0A3. Tel.: +1 (778) 782 8538; fax: +1 (778) 782 7514.
E-mail address: mbahrami@sfu.ca (M. Bahrami).

0017-9310/$ - see front matter © 2012 Elsevier Ltd. All rights reserved.
http://dx.doi.org/10.1016/j.ijheatmasstransfer.2012.12.019

Nomenclature

a	radius of adsorbent particle (m)
Bi_m	mass transfer Biot number, $h_m a/D$
c	adsorbate concentration (mol/m^3)
$\bar{c}$	total amount of adsorbate within the adsorbent particle (mol/m^3)
c^*	non-dimensional adsorbate concentration distribution
c_0	initial adsorbate concentration (mol/m^3)
c_∞	equilibrium adsorbate concentration, bulk concentration (mol/m^3)
C	electrical capacitance (F)
D	mass diffusivity (m^2/s)
D_{ij}	binary mass diffusion (m^2/s)
Fo	mass Fourier number, tD/a^2
h_m	mass transfer coefficient (m/s)
i	electric current (A)
m_t/m_∞	non-dimensional total amount of adsorbate within the adsorbent particle
r	radial coordinate
R	electrical resistance (Ω)
t	time (s)
V	electric potential (V)
$\forall$	volume (m^3)

Greek symbols

β_n	roots of characteristic equation, Eq. (13)
ε	porosity
η	non-dimensional coordinate, r/a
ω	adsorbate uptake, (kg adsorbate/kg dry adsorbent)
ω_{eq}	equilibrium adsorbate uptake, (kg adsorbate/kg dry adsorbent)

The main objective of this study, as a fundamental block to resolve the issues currently facing ACS, is to develop an in-depth understanding of adsorbate diffusion phenomenon within the adsorbent beds. To this end, a new compact closed-form relationship is developed to determine both adsorbate uptake rate and the mass diffusivity coefficient of adsorbent–adsorbate pairs. The proposed model is verified with experimental data collected from other sources.

2. Pertinent literature

There are several experimental techniques to measure the adsorbate uptake rate and the mass diffusivity reported in the literature, including, infrared spectroscopy, chromatography, nuclear magnetic resonance (NMR) and gravimetric methods, to name a few. More detail on measurement techniques are available elsewhere, e.g. [18]. A commonly used method is thermal gravimetric technique [18]. A thermogravimetric apparatus consists of an electrical furnace, crucible, and microbalance. The dried adsorbent particles are placed in the crucible which is located at the center of the furnace; it is also connected to the microbalance. To run a test, the furnace is set at a specific temperature and the adsorbate flows inside the furnace chamber. Simultaneously, the dried adsorbent particles start to adsorb adsorbate under the adsorption isotherm process and the microbalance measures the variation of the adsorbent mass over time. This method is a time-consuming method but there is almost no technical difficulty [19]. However, the measurement does not directly yield the mass diffusivity coefficient. To obtain the value of the mass diffusivity, an appropriate analytical adsorption model is needed for the analysis. By assuming a value for the mass diffusivity, a corresponding adsorbate uptake curve can be found using the analytical model. Then, it is compared to the experimental adsorbate uptake curve. The value of the mass diffusivity in the analytical model which provides the best match with the experimental result is taken as the true value of the mass diffusivity of the adsorbent–adsorbate pair at a specific pressure and temperature [19,20]. Accuracy of this method increases by developing a proper analytical model that can predict the mass diffusivity of adsorbent–adsorbate pairs under different operating conditions.

In general, the adsorbate uptake includes a number of physical processes, adsorbate transfer from the bulk gas to the adsorbent exterior surface, called gas-side resistance, diffusion of the adsorbate molecules to the pore surface of adsorbent particle, called solid-side resistance, and a resistance associated with the adsorption process itself. Often the last two resistances are more important than the first one [20–24]. Due to these factors, different mathematical models for the adsorption kinetics under different boundary conditions have been developed. Crank [25], and Karger and Ruthven [26] developed two different models for the concentration distribution of adsorbate within a spherical micropore adsorbent particle based on:

- Isothermal adsorption with constant concentration on the surface of adsorbent.
- Isothermal adsorption with solid-side resistance on the surface of adsorbent.

Later, Lee and Ruthven [27] developed a non-isothermal adsorption model with solid-side mass resistance for highly diffusive and/or reactive adsorbent–adsorbate pairs. Ni et al. [19] measured the water uptake rate of silica gel under different operating temperatures using thermogravimetric measurements. Then, they calculated the mass diffusivity of silica gel–water using two series-based models, namely the isothermal model with solid-side mass transfer resistance and the non-isothermal model with solid-side heat and mass transfer resistances. Their curve-fitted to the experimental data indicated that both models yield the same results because the tests were conducted under the adsorption isotherm process. Furthermore, Gurgel et al. [28] studied the water uptake rate of silica gel particles with three different diameters under the adsorption isotherm process. They used the isothermal model with no solid-side mass transfer resistance on the surface of adsorbent to predict the mass diffusivity of silica gel–water pair; however, their model failed to accurately predict the experimental data.

In many applications, adsorbate concentration boundary layer on the surface of adsorbent particle cannot be neglected and the solid-side resistance should be considered. For such problems, the solution of an isothermal process with the solid-side resistance is available in [26,27,29]. In case of negligible solid-side resistance, the solution converges to the isothermal adsorption with constant concentration on the surface of adsorbent.

Besides, several numerical simulations have been conducted by different researchers. Pesaran et al. [20] and San et al. [30,31] numerically investigated the effects of solid-side mass transfer resistance on the adsorption of water vapor by a packed bed of silica gel adsorbent. The challenges associated with the numerical simulation of adsorption phenomenon are its unsteady nature, time-consuming procedure, and iterative method to find the

accurate mass diffusivity of adsorbent–adsorbate pairs. Therefore, using an analytical model that can provide the mass diffusivity of adsorbent–adsorbate pairs in less time is preferred.

Most of the available analytical solutions in the open literature are based on series-solutions with non-linear characteristic equations to find both the adsorbate uptake rate by spherical micropore adsorbent particle and the mass diffusivity of adsorbent–adsorbate pairs. In the following sections, a new compact closed-form relationship has been developed based on the concept of resistance–capacitance (RC) model. The proposed relationship is compared with the available analytical solution, and later on, is applied to the experimental data reported by Ni et al. [19] and Gurgel et al. [28] to find the adsorbate uptake rate and the mass diffusivity of silica gel–water pair under various operating temperatures and silica gel sizes. The proposed model is general and can be applied to other adsorbent–adsorbate pairs such as activated carbon–methanol and zeolite–water.

3. Problem definition

In this study, a unit cell approach is adopted by considering a single spherical micropore adsorbent particle as the representative of the whole packed bed of adsorbent particles. The unit cell (or basic cell) is the smallest volume, which can represent characteristics of the entire microstructure [32]. Fig. 1 shows a schematic of a spherical micropore adsorbent particle with the solid-side resistance on the surface of the adsorbent.

To simplify the analysis, it is assumed that the initial adsorbate concentration distribution within the adsorbent particle is uniform, c_0, and is in equilibrium with the gaseous phase adsorbate. A sudden change in the concentration of gaseous adsorbate leads to adsorbate diffusion through/from the adsorbent particle vs. time. In this study, it is assumed that:

- Adsorbate uptake rate is controlled by the diffusion mass transfer.
- Constant temperature (isothermal) process during the adsorption/desorption time.
- Constant mass diffusivity [33].
- Solid-side resistance on the surface of spherical adsorbent.
- Radial diffusion of adsorbate within the adsorbent.

4. Mathematical model

Based on the assumptions made in Section 3, the mass balance for a single spherical adsorbent particle in spherical coordinate system can be expressed as follows [25,34]:

$$\frac{\partial c}{\partial t}=\frac{D}{r^2}\frac{\partial}{\partial r}\left(r^2\frac{\partial c}{\partial r}\right) \tag{1}$$

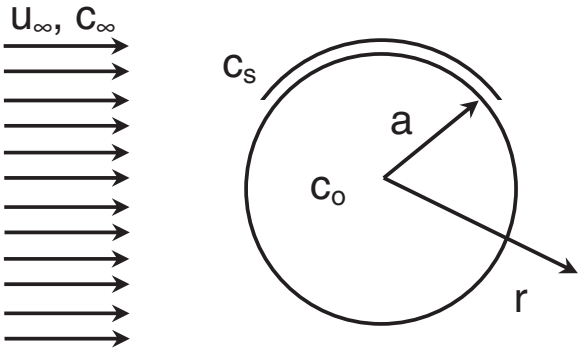

Fig. 1. A schematic of micropore adsorbent particle with solid-side resistance.

For a sudden change in the adsorbate concentration around the adsorbent particle, initial and boundary conditions are:

$$t=0,\quad c=c_0 \tag{2}$$

$$r=0,\quad \left.\frac{\partial c}{\partial r}\right|_{r=0}=0 \tag{3}$$

$$r=a,\quad h_m(c_\infty-c_s)=D\left.\frac{\partial c}{\partial r}\right|_{r=a} \tag{4}$$

The total amount of adsorbate uptake by the spherical adsorbent particle is:

$$\bar{c}(t)=\frac{3}{a^3}\int_0^a cr^2dr \tag{5}$$

Using the following variables Eqs. (1)–(5) can be non-dimensionalized.

$$c^*=\frac{c-c_0}{c_\infty-c_0},\quad \eta=\frac{r}{a},\quad Fo=\frac{tD}{a^2},\quad Bi_m=\frac{h_m a}{D} \tag{6}$$

where Fo and Bi_m are the mass Fourier number and the mass transfer Biot number, respectively. Note that Fo is the ratio of the diffusion mass transfer to the rate of mass storage, and Bi_m is the ratio of the convective to the diffusive mass transfer within the solid body. Bi_m is generally defined for the transient mass transfer. Eqs. (7)–(10) show the non-dimensional governing equation as well as initial and boundary conditions.

$$\frac{\partial c^*}{\partial Fo}=\frac{1}{\eta^2}\frac{\partial}{\partial \eta}\left(\eta^2\frac{\partial c^*}{\partial \eta}\right) \tag{7}$$

$$Fo=0,\quad c^*=0 \tag{8}$$

$$\eta=0,\quad \left.\frac{\partial c^*}{\partial \eta}\right|_{\eta=0}=0 \tag{9}$$

$$\eta=1,\quad Bi_m(1-c_s^*)=\left.\frac{\partial c^*}{\partial \eta}\right|_{\eta=1} \tag{10}$$

The non-dimensional total amount of adsorbate uptake by the adsorbent particle is:

$$\frac{m_t}{m_\infty}=\frac{\bar{c}-c_0}{c_\infty-c_0}=3\int_0^1 c^*\eta^2d\eta \tag{11}$$

where m_t and m_∞ are the adsorbed mass of adsorbate at time t and $t\to\infty$, respectively.

Crank [25] and Ruthven et al. [26,29] solved Eq. (7) by method of separation of variables under the same initial and boundary conditions defined in Eqs. (8)–(10). Eq. (12) gives the concentration distribution within the spherical adsorbent particle [25–27,29].

$$c^*=\frac{2Bi_m}{\eta}\sum_{n=1}^{\infty}\frac{\exp(-\beta_n^2Fo)}{\beta_n^2+Bi_m(Bi_m-1)}\frac{\sin(\beta_n\eta)}{\sin(\beta_n)} \tag{12}$$

where β_n is the roots of Eq. (13).

$$\beta_n\cot(\beta_n)+Bi_m-1=0 \tag{13}$$

The total amount of adsorbate uptake by the spherical adsorbent particle is calculated as follows:

$$\frac{m_t}{m_\infty}=1-\sum_{n=1}^{\infty}\frac{6Bi_m^2\exp(-\beta_n^2Fo)}{\beta_n^2\left(\beta_n^2+Bi_m(Bi_m-1)\right)} \tag{14}$$

The series solution in Eq. (12) has two asymptotes,

- $Bi_m\to 0$ (no diffusive resistance inside the adsorbent, i.e., lumped capacitance),
- $Bi_m\to\infty$ (no solid-side resistance on the surface of adsorbent).

Table 1
Roots of Eq. (13) for different mass transfer Biot numbers.

Roots of Eq. (13)	Mass transfer Biot number, Bi_m							
	0	0.1	0.5	1	2	5	10	∞
β_1	0	0.5423	1.1656	$\pi/2$	2.0287	2.5704	2.8363	π
β_2	4.4934	4.5157	4.6042	$3\pi/2$	4.9132	5.3540	5.7172	2π
β_3	7.7253	7.7382	7.7899	$5\pi/2$	7.9786	8.3029	8.6587	3π
β_4	10.9041	10.9133	10.9499	$7\pi/2$	11.0855	11.3348	11.6532	4π
β_5	14.0662	14.0733	14.1017	$9\pi/2$	14.2074	14.4079	14.6869	5π
β_6	17.2208	17.2266	17.2498	$11\pi/2$	17.3364	17.5034	17.7480	6π
β_7	20.3713	20.3762	20.3958	$13\pi/2$	20.4692	20.6120	20.8282	7π
β_8	23.5195	23.5237	23.5407	$15\pi/2$	23.6043	23.7289	23.9218	8π
β_9	26.6661	26.6698	26.6848	$17\pi/2$	26.7409	26.8514	27.0250	9π
β_{10}	29.8116	29.8149	29.8284	$19\pi/2$	29.8786	29.9778	30.1353	10π

In the limiting case of $Bi_m \to 0$ (lumped capacitance model), the resistance to diffusion within the solid is much less than the resistance to convective mass transfer from the solid-side resistance. Therefore, the assumption of a uniform concentration distribution within the spherical adsorbent particle is reasonable [35]. In this case, β_n is small and the first term in the series solution, Eq. (12), would suffice for calculations [26,29]. Eqs. (15)–(18) show the solution, where $Bi_m \to 0$:

$$\cot(\beta_1) \approx \frac{1}{\beta_1} - \frac{\beta_1}{3} - \frac{\beta_1^3}{45} - \dots \tag{15}$$

$$\beta_1 \cot(\beta_1) - 1 \approx -\frac{\beta_1^2}{3} = -Bi_m \quad \Rightarrow \quad \beta_1^2 = 3Bi_m \tag{16}$$

$$c^* = \exp(-3Bi_m Fo) \tag{17}$$

$$\frac{m_t}{m_\infty} = 1 - \exp(-3Bi_m Fo) \tag{18}$$

In the limiting case of $Bi_m \to \infty$ (no solid-side resistance on the surface of adsorbent), the solution yields to the solution of isothermal adsorption with constant concentration on the surface of the adsorbent particle. Eq. (19) gives the adsorbate concentration distribution within the spherical adsorbent particle at the limit, where $Bi_m \to \infty$:

$$c^* = 1 + \frac{2}{\pi\eta}\sum_{n=1}^{\infty}\frac{(-1)^n}{n}\exp(-n^2\pi^2 Fo)\sin(n\pi\eta) \tag{19}$$

and the total amount of adsorbate uptake by the spherical adsorbent particle for $Bi_m \to \infty$ is:

$$\frac{m_t}{m_\infty} = 1 - \frac{6}{\pi^2}\sum_{n=1}^{\infty}\frac{\exp(-n^2\pi^2 Fo)}{n^2} \tag{20}$$

Roots of Eq. (13) for the first 10 terms of the series solution, Eq. (12), are tabulated in Table 1 for different mass transfer Biot numbers.

The total amount of adsorbate uptake by the spherical adsorbent particle, Eq. (14), vs. *Fo* number is shown in Fig. 2. As shown in Fig. 2, the adsorbate uptake rate increases by increasing Bi_m at constant *Fo*.

In addition, Fig. 2 indicates the effects of the solid-side resistance on the amount of adsorbate uptake. In case of no solid-side resistance on the surface of adsorbent, $Bi_m \to \infty$, amount of adsorbate uptake is much higher than that of the high solid-side resistance cases, $Bi_m \to 0$.

The shown values in Fig. 2 are calculated using the first 10 terms of the series solution, Eq. (14). As mentioned in Section 2, finding the mass diffusivity of adsorbent–adsorbate pair by the gravimetric method is an iterative and time consuming procedure. One way to simplify this procedure is to truncate the series solution, Eq. (14). Fig. 3 shows the effect of truncating the series solution, Eq. (14), on the adsorbate uptake curve for different Bi_m.

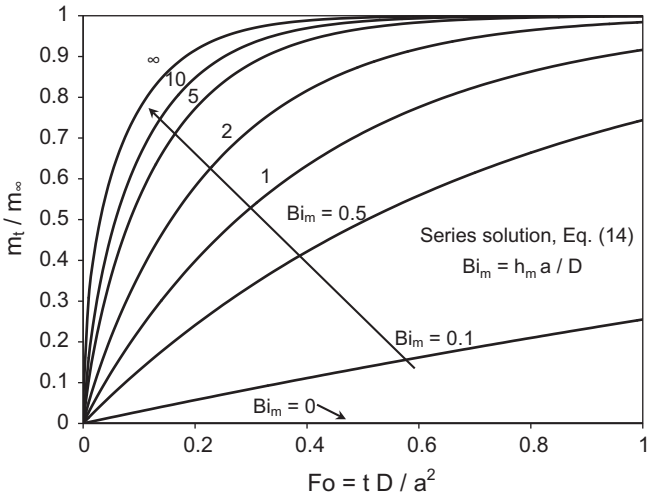

Fig. 2. Total amount of adsorbate uptake vs. mass Fourier number, Eq. (14).

Fig. 3 clearly indicates that by increasing Bi_m, the effect of number of terms in the series solution, Eq. (14), on the calculated adsorbate uptake becomes more important. The maximum relative difference between the adsorbate uptake curves calculated by the limited number of terms in the series solution, Eq. (14), with respect to the first 10 terms of the series solution is summarized in Table 2.

As shown in Table 2, having a closed-form solution for different Bi_m with only the first few terms of the series solution is not accurate; the first 10 terms of series solution is considered in all calculations.

5. Proposed compact closed-form relationship

As discussed in Section 4, the analytical adsorbate uptake calculated by the series solution, Eq. (14), cannot be easily used for the entire range of Bi_m, see Fig. 3. Eq. (21) shows the classical linear driving force (LDF) solution proposed by Glueckauf [36] which is one of the classical solutions used in adsorbate uptake modeling.

$$\frac{m_t}{m_\infty} = 1 - \exp(-15Fo) \tag{21}$$

Eq. (21) corresponds to Eq. (20) which is derived for $Bi_m \to \infty$ with an average relative difference of 1.34%. Eq. (21) is widely used in prediction of both adsorbate uptake rate by the adsorbent

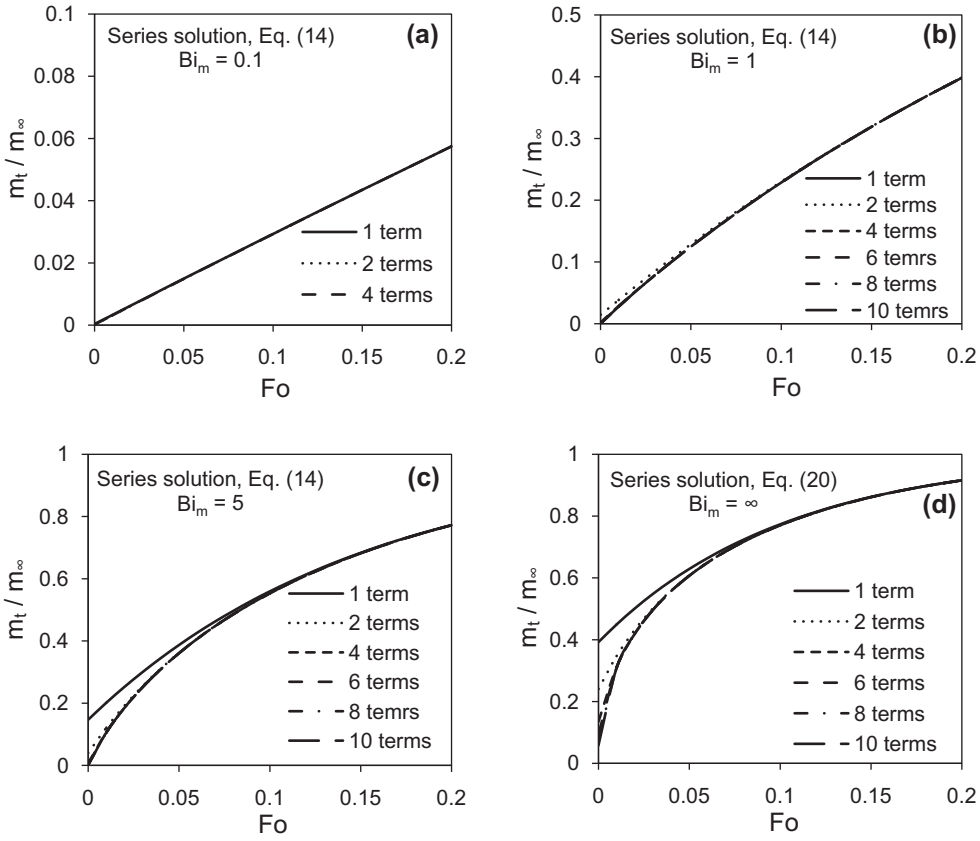

Fig. 3. Effect of truncating the series solution on the adsorbate uptake curve for different Bi_m.

Table 2
Maximum relative difference between the adsorbate uptake curves calculated by finite number of terms of the series solution, Eq. (14), compared with the first 10 terms.

No. of terms in Eq. (14)	Mass transfer Biot number, Bi_m			
	0.1	1	5	∞
1	4.1%	38.7%	90.6%	45.6%
2	0.36%	3.6%	14.14%	12.4%
4	2.5×10^{-3}%	0.09%	0.46%	0.86%
6	2.0×10^{-4}%	2.2×10^{-3}%	0.01%	0.04%
8	3.4×10^{-6}%	3.8×10^{-5}%	2.2×10^{-4}%	9.2×10^{-4}%

particle and the mass diffusivity of adsorbent–adsorbate pairs [15,37–39]. However, its application range is limited to $Bi_m \to \infty$. Moreover, it is not valid for small mass transfer Biot numbers [20].

A careful observation of the adsorbate uptake in spherical adsorbent particle, shown in Fig. 2, reveals similarities with charging of an electrical capacitor. Therefore, we propose a solution for the mass transfer using the solution of the corresponding electrical circuit. The analogous parameters between the heat/mass transfer and the electrical circuit are summarized in Table 3.

Diffusion in micropore materials can be assumed as a quasi-steady state process. As a result, one can use a resistance–capacitance (RC) model to simulate the charging of a spherical micropore adsorbent particle. Shown in Fig. 4 is a simple charging circuit of a capacitor and an equivalent electrical circuit for the adsorbate uptake by the spherical adsorbent particle based on the analogy between the mass transfer and the electrical circuit.

The charging behavior of the capacitor shown in Fig. 4a is [40]:

$$\frac{V_{\text{capacitor}}(t)}{V_0} = 1 - \exp\left(-\frac{t}{\text{RC}}\right) \tag{22}$$

Table 3
Analogous parameters between heat/mass transfer and electrical circuit.

	Mass transfer	Heat transfer	Electrical circuit
Potential	Δc (mol/m^3)	ΔT (K)	V (V)
Flux	J'' (mol/m^{2}s)	q'' (W/m^2)	i (A)
Resistance	$\frac{1}{h_m \varepsilon A}, \frac{a}{D \varepsilon A}$ (s/m^3)	$\frac{1}{hA}, \frac{a}{kA}$ (K/W)	R (Ω)
Capacitance	$\varepsilon \forall$(m^3)	mc_p (J/K)	C (F)

In the same way, the adsorbate uptake by the spherical micropore adsorbent particle corresponding to the electrical circuit is shown in Fig. 4b, where C is the mass capacitance, R_1 is the solid-side resistance, and R_2 is the diffusive resistance within the spherical micropore adsorbent particle, respectively.

With reference to Table 3, the mass capacitance of a spherical micropore adsorbent particle is:

$$C = \frac{4}{3}\pi\varepsilon a^3 \tag{23}$$

where, ε and a are the porosity and the radius of the micropore adsorbent particle, respectively. Moreover, the solid-side resistance, R_1, and the diffusive resistance within the spherical micropore adsorbent particle, R_2, are shown in Table 4.

α in the diffusive resistance, Table 4, is a constant and will be calculated by using the linear driving force (LDF) model. The total resistance can be found by summation of the resistances, see Eq. (24).

$$R = R_1 + R_2 \tag{24}$$

Eq. (25) shows the simplified multiplication of the mass capacitance, Eq. (23), and the total resistance, Eq. (24).

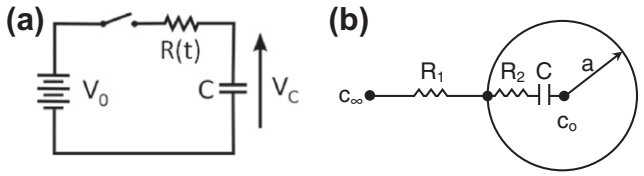

Fig. 4. (a) A simple resistor–capacitor circuit to charge a capacitor [40] (b) Equivalent electrical circuit for the adsorbate uptake by the spherical adsorbent particle.

Table 4
Analogy between mass transfer resistance and electrical resistance.

Resistance	Mass transfer (s/m^3)	Electrical circuit
Solid-side resistance	$1/(4\pi\varepsilon a^2 h_m)$	R
Diffusive resistance	$1/(4\pi\varepsilon\alpha a D)$	R_2

$$RC = \frac{1.0 + \frac{h_m a}{\alpha D}}{3\frac{h_m}{a}} \tag{25}$$

By substituting Eq. (25) in Eq. (22) and using the analogy between the mass transfer and the electrical circuit, the final RC model solution for charging a spherical adsorbent particle becomes:

$$\frac{m_t}{m_\infty} = 1 - \exp\left(-\frac{3\frac{h_m t}{a}}{1.0 + \frac{h_m a}{\alpha D}}\right) \tag{26}$$

Eq. (26) can be further simplified by substituting the non-dimensional parameters defined in Eq. (6). Thus, the total amount of adsorbate uptake by a spherical adsorbent particle becomes:

$$\frac{m_t}{m_\infty} = 1 - \exp\left(-\frac{3Bi_m Fo}{1.0 + \frac{Bi_m}{\alpha}}\right) \tag{27}$$

Eq. (27) has two asymptotes quite similar to those of Eq. (14). In the limiting case of $Bi_m \to 0$ (lumped capacitance model), Eq. (27) yields the exact same result of Eq. (18). In the limiting case of

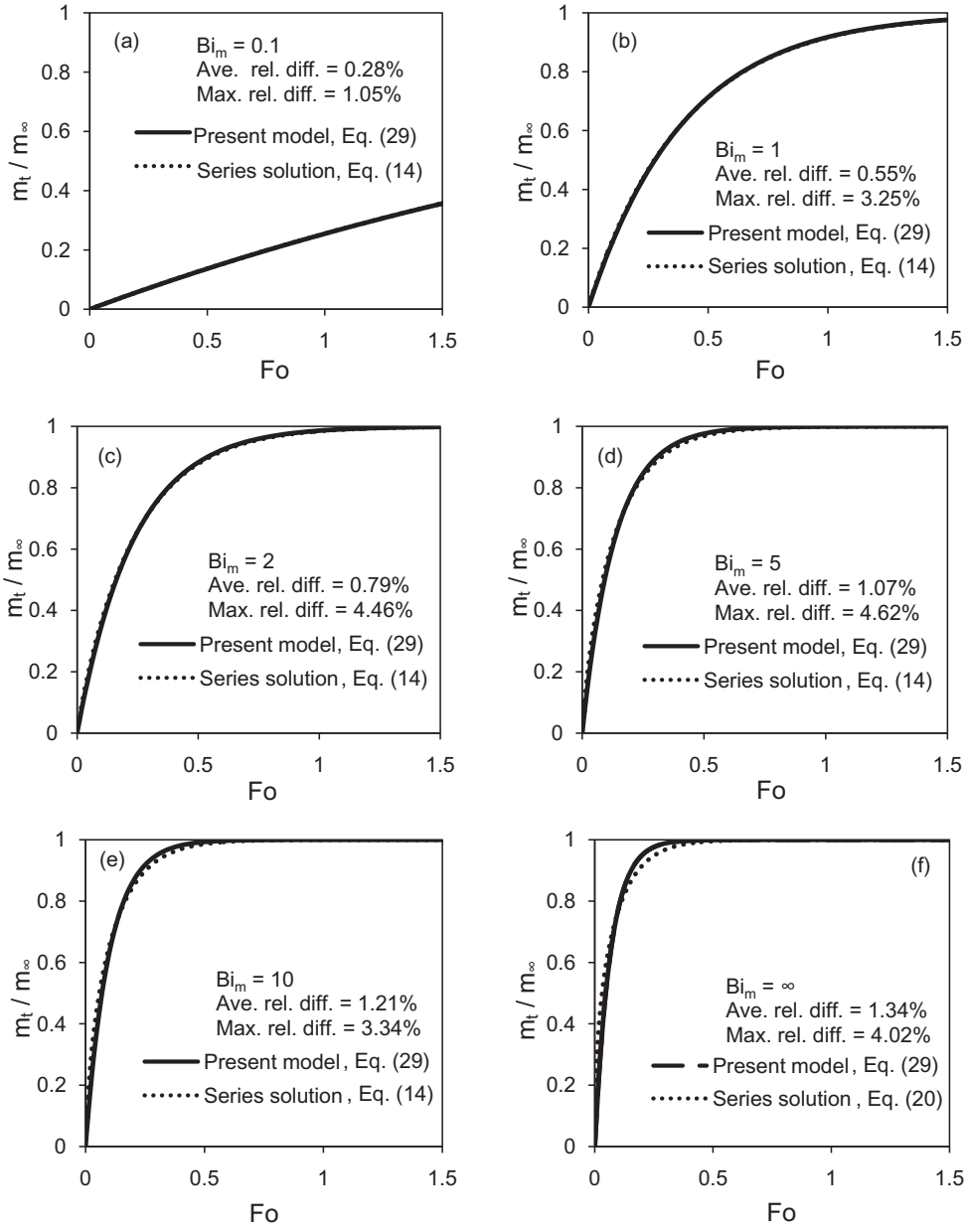

Fig. 5. Comparison between the present compact model and the series solution for (a) $Bi_m = 0.1$, (b) $Bi_m = 1$, (c) $Bi_m = 2$, (d) $Bi_m = 5$, (e) $Bi_m = 10$, and (f) $Bi_m \to \infty$.

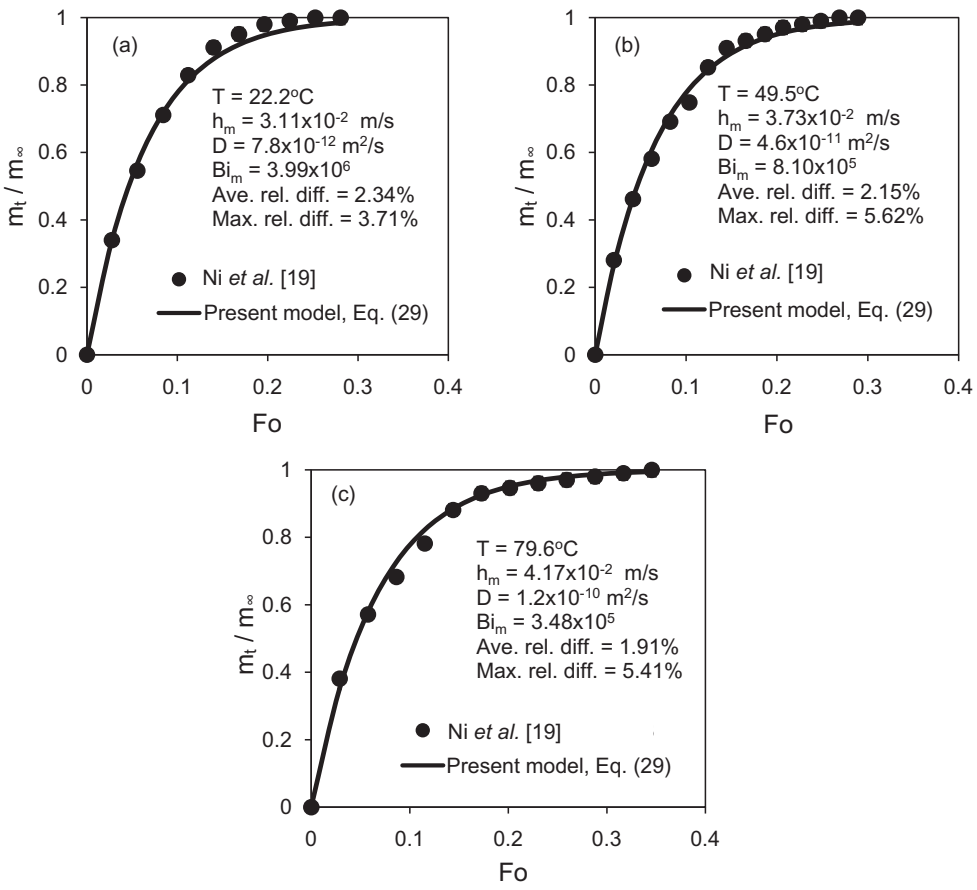

Fig. 6. Total amount of water uptake by 2 mm silica gel adsorbent particles at temperatures of 22.2, 49.5 and 79.6 °C.

$Bi_m \to \infty$ (no solid-side resistance on the surface of adsorbent), Eq. (27) yields Eq. (28) which should be equivalent to the linear driving force (LDF) model, i.e., Eq. (21).

$$\frac{m_t}{m_\infty} = 1 - \exp(-3\alpha Fo) \tag{28}$$

As a result, α in Eq. (28) should be equal to five. Hence, the final closed-form relationship for the adsorbate uptake by the spherical micropore adsorbent particle for the entire range of mass transfer Biot numbers is:

$$\frac{m_t}{m_\infty} = 1 - \exp\left(-\frac{3Bi_m Fo}{1.0 + 0.2Bi_m}\right) \tag{29}$$

A comparison between the present model, Eq. (29), and the analytical series solution for different values of Bi_m are presented in Fig. 5. It can be seen that the present model has a good agreement with the analytical series solution for the entire range of mass transfer Biot numbers. The average relative difference between the present model and the analytical series solution varies between 0% and 1.34% for different Bi_m. It should be mentioned that the maximum relative difference in all cases are reported for $Fo > 0.1$.

To find the mass diffusivity of the adsorbent–adsorbate pairs by using experimental data of the gravimetric method, the mass transfer coefficient, h_m, should be known. To this end, an analogy between heat and mass transfer can be established under specific conditions, commonly referred to as Chilton–Colburn J-factor analogy [41]. To establish a valid heat–mass convection analogy, the mass flux should be low such that the mass transfer between the fluid and the surface does not affect the flow velocity [33]. In case of diffusion within the micropore materials, the low mass flux process assumption is valid and, as a result, the analogy between the convective heat and mass transfer is reasonable. Thus, Eq. (30) developed for the convective heat transfer around a spherical particle, can be applied to convective mass transfer around a spherical micropore particle, Eq. (31) [42].

$$Nu = \frac{h(2a)}{k} = 2.0 + 0.6\mathrm{Re}^{\frac{1}{2}}\mathrm{Pr}^{\frac{1}{3}} \quad 0 \leqslant \mathrm{Re} < 200, \quad 0 \leqslant \mathrm{Pr} < 250 \tag{30}$$

$$Sh = \frac{h_m(2a)}{D_{ij}} = 2.0 + 0.6\mathrm{Re}^{\frac{1}{2}}Sc^{\frac{1}{3}} \quad 0 \leqslant \mathrm{Re} < 200, \quad 0 \leqslant Sc < 250 \tag{31}$$

where Sh is the Sherwood number, Re is the Reynolds number based on the particle diameter and Sc is the Schmidt number which is given by Eq. (32), respectively.

$$Sc = \frac{v}{D_{ij}} \tag{32}$$

where D_{ij} is the binary mass diffusivity of ideal gas mixture. Eq. (33) gives the binary mass diffusivity of water vapor in the air [43].

$$D_{\mathrm{H_2O-air}}(T,P) = 1.87 \times 10^{-10}\frac{T^{2.072}}{P} \quad \left(\frac{m^2}{s}\right) \quad 280K \leqslant T < 450K \tag{33}$$

where P is the total pressure in atmosphere and T is the mixture temperature in K, respectively. The Schmidt number for diffusion of water vapor in the air is about 0.6 [35]. At the end, the mass transfer coefficient, h_m, is given by Eq. (34).

$$h_m = D_{ij}(2.0 + 0.6\mathrm{Re}^{\frac{1}{2}}Sc^{\frac{1}{3}})/(2a) \quad (34)$$

There is no relationship to calculate the mass transfer Biot number directly. Hence, a value for the mass diffusivity should be found based on the experimental data. Accordingly, the mass transfer Biot number can be found using Eqs. (6) and (34).

$$Bi_m = D_{ij}(2.0 + 0.6\mathrm{Re}^{\frac{1}{2}}Sc^{\frac{1}{3}})/(2D) \quad (35)$$

6. Results and discussion

The proposed closed-form relationship is a general transient mass diffusion model applicable to the entire range of Bi_m and can be used in a wide range of applications to predict the transient adsorption/desorption processes in adsorption cooling systems (ACS) and to calculate the mass diffusivity of micropore adsorbent–adsorbate pairs.

6.1. Non-equilibrium adsorbate uptake in ACS

One of the applications of the present model, Eq. (29), is to predict the total amount of adsorbate uptake during the adsorption/desorption processes. The non-equilibrium amount of adsorbate uptake during the adsorption/desorption processes is mainly expressed by ω which is the ratio of mass of adsorbate to the mass of dry adsorbent [15,37–39]. To make the present model, Eq. (29), compatible to this definition, Eq. (36) is introduced.

$$\frac{m_t}{m_\infty} = \frac{m_t/m_{\text{dry adsorbent}}}{m_\infty/m_{\text{dry adsorbent}}} = \frac{\omega}{\omega_{eq}} = 1 - \exp\left(-\frac{3Bi_mFo}{1.0 + 0.2Bi_m}\right) \quad (36)$$

where ω_{eq} is the equilibrium adsorbate uptake at specific temperature and pressure. To implement Eq. (36) in the dynamic modeling of ACS thermodynamic cycle, adsorbate uptake rate is required. Eq. (37) gives the adsorption uptake rate by differentiating Eq. (36) with respect to time.

$$\frac{d\omega}{dt} = \frac{3Bi_m}{1.0 + 0.2Bi_m}\frac{D}{a^2}(\omega_{eq} - \omega) \quad (37)$$

Similarly, the adsorbate uptake rate based on the LDF model, Eq. (21), is given by Eq. (38) that is commonly used in dynamic modeling of ACS thermodynamic cycles and is valid for $Bi_m \to \infty$ (no solid-side resistance on the surface of adsorbent) [15,37–39].

$$\frac{d\omega}{dt} = \frac{15D}{a^2}(\omega_{eq} - \omega) \quad (38)$$

It is noteworthy that the proposed adsorbate uptake rate, Eq. (37), is as convenient-to-use as the LDF adsorbate uptake rate, Eq. (38); also it is applicable to the entire range of mass transfer Biot numbers. Eq. (37) can be easily applied to dynamic modeling of ACS thermodynamic cycles for different mass transfer Biot numbers.

6.2. Calculation of mass diffusivity of spherical micropore adsorbent–adsorbate pair

The other application of the present model, Eq. (29), is to find the mass diffusivity of adsorbent–adsorbate pairs in ACS applications. In this study, the experimental data of water uptake by silica gel particles reported by Ni et al. [19] and Gurgel et al. [28] are used to find the mass diffusivity of silica gel–water pair by the present model, Eq. (29).

Ni et al. [19], used a thermal gravimetrical apparatus to measure the total water uptake (adsorbate) in a 2 mm silica gel

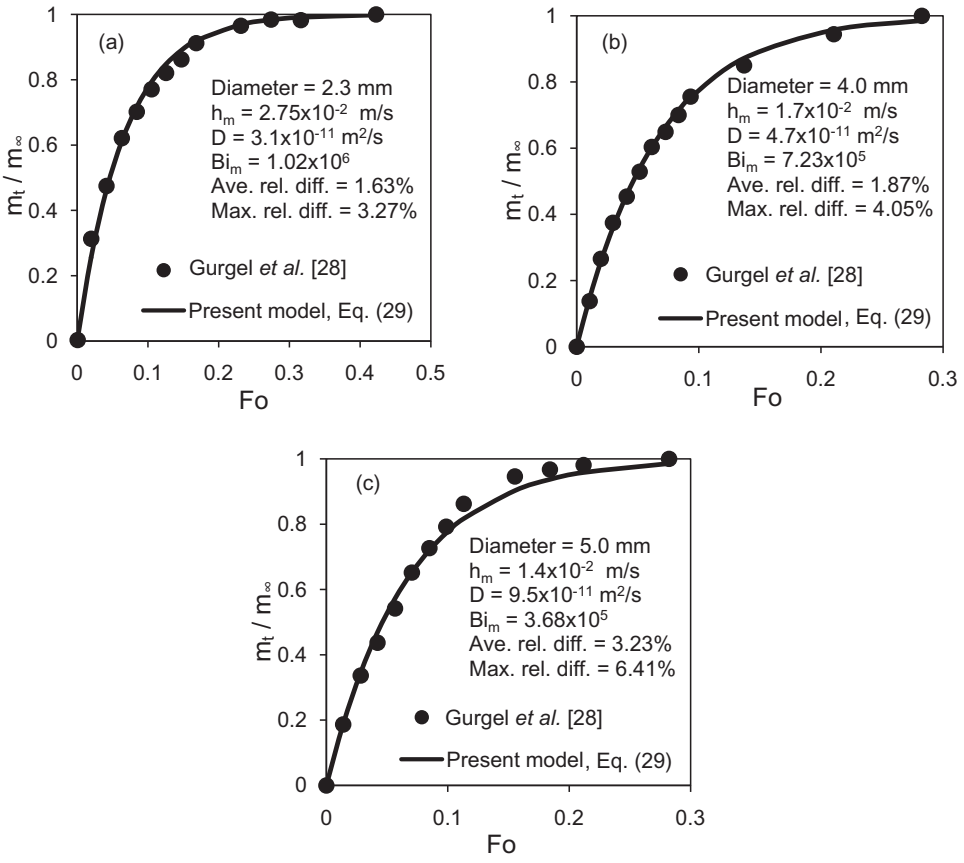

Fig. 7. Total amount of water uptake by silica gel adsorbent particles with diameter of (a) 2.3 mm, (b) 4.0 mm, and (c) 5.0 mm.

adsorbent particles under atmospheric pressure and different operating temperatures. The silica gel particles were placed far from the others with enough spacing to minimize effects of the interaction among them. The moist air average velocity in the experimental work of [19] was 9.3×10^{-3} m/s and the maximum uncertainty for the mass diffusivity was 25%.

Shown in Fig. 6 is the total amount of water uptake by the silica gel adsorbent particles in operating temperatures of 22.2, 49.5 and 79.6 °C.

Fig. 6 shows that the water uptake curve calculated by the present model is in excellent agreement with the experimental data of [19] under the assumption of constant specific mass diffusivity. As it can be seen in Fig. 6, by increasing the operating temperature, the mass transfer coefficient, h_m, and the mass diffusivity, D, of silica gel–water pair increases while the mass transfer Biot number decreases, which is mainly due to a higher increase in the mass diffusivity than the mass transfer coefficient.

The present model, also, is applied to determine the mass diffusivity of the working pair in the experimental data of Gurgel et al. [28] for three different sizes of silica gel–water pairs at a constant temperature of 22 °C and atmospheric pressure. The uncertainty analysis and the moist air average velocity in the experimental work of Gurgel et al. [28] were not reported. To perform the analysis, the same average velocity of 9.3×10^{-3} m/s reported by Ni et al. [19] is used in the calculations. Gurgel et al. [28] used the model of adsorbate uptake with constant concentration on the surface of adsorbent. Fig. 7 shows the water uptake curves produced by the present model, Eq. (29), for spherical silica gel adsorbent particles with diameters of 2.3, 4.0 and 5.0 mm at temperature of 22 °C [28].

As shown in Fig. 7, the water uptake curves calculated by the present model under the constant mass diffusivity have a good agreement with the experimental data reported by Gurgel et al. [28]. The maximum and average relative difference between the present model and the experimental data are 3.3% and 1.6% for 2.3 mm silica gel particle, 4.0% and 1.9% for 4.0 mm silica gel particle and 7.2% and 3.0% for 5.0 mm silica gel particle.

7. Summary and conclusions

In this study the adsorbate diffusion within the spherical micropore adsorbent particle with the solid-side resistance on the surface of adsorbent was investigated. Using an analogy between the mass transfer and electrical circuits, a resistance–capacitance (RC) compact model has been introduced to simulate behavior of adsorbate uptake by spherical micropore adsorbent particles. Calculated adsorbate uptake curves by the proposed model, Eq. (29), and the series solution, Eq. (14), showed a good agreement. The proposed model was also used to determine both adsorbate uptake rate and the mass diffusivity coefficient of adsorbent–adsorbate pairs based on the measured adsorbate uptake curves by Ni et al. [19] and Gurgel et al. [28].

The following are the highlights of the present study:

- The proposed new model has a good agreement with the analytical series solution with an average relative difference of 1.34% for the entire range of mass transfer Biot numbers.
- Non-equilibrium adsorbate uptake rate was proposed for calculation of uptake rate during the adsorption/desorption processes in ACS for different values of mass transfer Biot numbers.
- The proposed RC-based model is able to determine the mass diffusivity of spherical micropore adsorbent–adsorbate pairs using a compact relationship compared to the existing analytical series solution.

Acknowledgments

The authors gratefully acknowledge the financial support of the Natural Sciences and Engineering Research Council of Canada (NSERC) through the Automotive Partnership Canada Grant No. APCPJ 401826-10.

References

[1] J. Caro, Diffusion in porous functional materials: Zeolite gas separation membranes, proton exchange membrane fuel cells, dye sensitized solar cells, Micropor. Mesopor. Mat. 125 (2009) 79–84.
[2] X. Yin, J. Wang, N. Chu, J. Yang, J. Lu, Y. Zhang, D. Yin, Zeolite L/carbon nanocomposite membranes on the porous alumina tubes and their gas separation properties, J. Membrane Sci. 348 (2010) 181–189.
[3] S.S. Kapdi, V.K. Vijay, S.K. Rajesh, R. Prasad, Biogas scrubbing, compression and storage: perspective and prospectus in Indian context, Renew. Energy 30 (8) (2005) 1195–1202.
[4] J.A. Ritter, A.D. Ebner, State-of-the-art adsorption and membrane separation processes for hydrogen production in the chemical and petrochemical industries, Separ. Sci. Technol. 42 (6) (2007) 1123–1193.
[5] S. Aguado, A.C. Polo, M.P. Bernal, J. Coronas, J. Santamaria, Removal of pollutants from indoor air using Zeolite membranes, J. Membrane Sci. 240 (2004) 159–166.
[6] S. Bhatia, A.Z. Abdullah, C.T. Wong, Adsorption of butyl acetate in air over silver-loaded Y and ZSM-5 zeolites: experimental and modeling studies, J. Hazard. Mater. 163 (2009) 73–81.
[7] M. Urbiztondo, I. Pellejero, A. Rodriguez, M.P. Pina, J. Santamaria, Zeolite-coated interdigital capacitors for humidity sensing, Sensor. Actuat. B-Chem. 157 (2011) 450–459.
[8] I. Sjoholm, V. Gekas, Apple shrinkage upon drying, J. Food Eng. 25 (1) (1995) 123–130.
[9] Z. Yusheng, K.P. Poulsen, Diffusion in potato drying, J. Food Eng. 7 (4) (1988) 249–262.
[10] A. Lopez, A. Iguaz, A. Esnoz, P. Virseda, Thin-layer drying behavior of vegetable wastes from wholesale market, Dry. Technol. 18 (4–5) (2000) 995–1006.
[11] R. Langer, New methods of drug delivery, Science (1990) 1527–1533.
[12] K.S. Soppimath, T.M. Aminabhavi, A.R. Kulkarni, W.E. Rudzinski, Biodegradable polymeric nanoparticles as drugdelivery devices, J. Control. Release 70 (1–2) (2001) 1–20.
[13] L.Z. Zhang, L. Wang, Performance estimation of an adsorption cooling system for automotive waste heat recovery, Appl. Therm. Eng. 17 (12) (1997) 1127–1139.
[14] Y.Z. Lu, R.Z. Wang, S. Jianzhou, M. Zhang, Y.X. Xu, J.Y. Wu, Performance of a diesel locomotive waste-heat-powered adsorption air conditioning system, Adsorption 10 (2004) 57–68.
[15] M. Verde, L. Cortes, J.M. Corberan, A. Sapienza, S. Vasta, G. Restuccia, Modeling of an adsorption system driven by engine waste heat for truck cabin A/C. Performance estimation for a standard driving cycle, Appl. Therm. Eng. 30 (2010) 1511–1522.
[16] R. Farrington, J. Rugh, Impact of vehicle air-conditioning on fuel economy, tailpipe emissions, and electric vehicle range, in: Proceeding of the Earth Technologies Forum, Washington, D.C., October 3, 2000.
[17] Z. Han, A. Fina, Thermal conductivity of carbon nanotubes and their polymer nanocomposites: a review, Prog. Polym. Sci. 36 (2011) 914–944.
[18] D.M. Ruthven, in: W.C. Conner, J. Fraissard (Eds.), Fluid Transport in Nanoporous Materials, Springer, Dordrecht, 2006, pp. 151–186.
[19] C.C. Ni, J.Y. San, Measurement of apparent solid-side mass diffusivity of a water vapor–silica gel system, Int. J. Heat Mass Transfer 45 (2002) 1839–1847.
[20] A.A. Pesaran, A.F. Mills, Moisture transport in silica gel packed beds-I theoretical study, Int. J. Heat Mass Transfer 30 (6) (1987) 1037–1049.
[21] J.W. Nienberg, Modeling of desiccant performance for solar-desiccant-evaporative cooling systems, M.S. Thesis, School of Engineering and Applied Science, University of California, Los Angeles, 1977.
[22] J.W. Clark, A.F. Mills, H. Buchberg, Design and testing of thin adiabatic desiccant beds for solar air conditioning applications, J. Sol. Energy Eng. 103 (1981) 89–91.
[23] C.E. Bullock, J.L. Threlkeld, Dehumidification of moist air by adiabatic adsorption, Trans. ASHRAE 72 (1966). Part I 301–313.
[24] F.E. Pla-Barby, G.C. Vliet, Rotary bed solid desiccant drying: An analytical and experimental investigation, in: ASME/AIChE 18th Natinal Heat Transfer Conference, San Diego, CA, 1979.
[25] J. Crank, The Mathematics of Diffusion, Oxford University Press, 1967.
[26] J. Karger, D.M. Ruthven, Diffusion in Zeolites and Other Microporous Solids, Wiley & Sons, Inc., 1992.
[27] L.K. Lee, D.M. Ruthven, Analysis of thermal effects in adsorption rate measurement, J. Chem. Soc. Faraday Trans. 75 (11) (1979) 2406–2422.
[28] J.M. Gurgel, L.S. Andrade, P.P.S. Couto, Apparent diffusivity of water in silica gel and NaX zeolite pellets, High Temp. High Press. 33 (2001) 435–439.
[29] D.M. Ruthven, Principles of Adsorption and Desorption Processes, John Wiley &Sons, Inc., 1984.

[30] J.Y. San, G.D. Jiang, Modeling and testing of a silica gel packed-bed system, Int. J. Heat Mass Transfer 37 (8) (1994) 1173–1179.
[31] J.Y. San, Y.C. Hsu, Adsorption of toluene on activated carbon in a packed bed, Int. J. Heat Mass Transfer 41 (21) (1998) 3229–3238.
[32] A. Tamayol, M. Bahrami, Parallel flow through ordered fibers: an analytical approach, ASME J. Fluid Eng. 132 (2010) 114502.
[33] Y. Cengel, Heat and Mass Transfer: A Practical Approach, third ed., McGraw-Hill Science, 2006.
[34] H.s. Carslaw, J.C. Jaeger, Conduction of Heat in Solids, Oxford University Press, 1947.
[35] F.P. Incropera, D.P. DeWitt, T.L. Bergman, A.S. Lavine, Fundamentals of Heat and Mass Transfer, sixth ed., Wiley, 2006.
[36] E. Glueckauf, Theory of chromatography: 10. Formulate for diffusion into spheres and their application to chromatography, J. Chem. Soc. Faraday Trans. 51 (1955) 1540.
[37] A. Sakoda, M. Suzuki, Fundamental study on solar powered adsorption cooling system, J. Chem. Eng. Jpn. 17 (1984) 52–57.
[38] L.Z. Zhang, L. Wang, Effects of coupled heat and mass transfers in adsorbent on the performance of a waste heat adsorption cooling unit, Appl. Therm. Eng. 19 (1999) 195–215.
[39] K.C. Chan, C.Y.H. Chao, G.N. Sze-To, K.S. Hui, Performance predictions for a new zeolite 13X/CaCl2 composite adsorbent for adsorption cooling systems, Int. J. Heat Mass Transfer 55 (2012) 3214–3224.
[40] T.L. Floyd, Electric Circuits Fundamentals, sixth ed., Prentice Hall, 2003.
[41] B.M. Suryavanshi, L.R. Dongre, Transport Phenomena, first ed., Nirali Prakashan, 2006. section: 15.1.3.
[42] W.E. Ranz, W.R. Marshall, Evaporation from drops, Chem. Eng. Prog. 48 (3) (1952) 141–146. 48(4), 173–180.
[43] M.W. DennyNi, J.Y. San, Air and Water: The Biology and Physics of Life's Media, Princeton University Press, 1993.